Contribution from the Department of Chemistry, University of Florence, Via Maragliano 75/77, 50144 Florence, Italy, Department of Energetics, University of Florence, Santa Marta, Florence, Italy, Institute of Chemical Sciences, University of Urbino, Urbino, Italy, and Department of Inorganic Chemistry, University of Valencia, C/Dr. Moliner 50, 46100 Burjassot, Valencia, Spain

# Thermodynamic and Structural Aspects of the Interaction between Macrocyclic Polyammonium Cations and Complexed Anions

Andrea Bencini,[1a] Antonio Bianchi,*[,1a] Paolo Dapporto,[1b] Enrique Garcia-España,*[,1c] Mauro Micheloni,[1d] José Antonio Ramirez,[1c] Piero Paoletti,*[,1a] and Paola Paoli[1b]

*Received August 6, 1991*

The interaction of polyprotonated forms of [3k]aneN$_k$ ($k$ = 7-12) macrocycles with the complexed anions $Fe(CN)_6^{4-}$, $Co(CN)_6^{3-}$, and $Pt(CN)_4^{2-}$ has been studied by potentiometry in 0.15 mol dm$^{-3}$ $NaClO_4$ solution at 298.15 K, and the stability constants of the second-sphere complexes formed have been determined. The interaction of $(H_k[3k]aneN_k)^{k+}$ ($k$ = 7-11) cations with $PtCl_6^{2-}$ and $Pt(CN)_4^{2-}$ has been followed by $^{195}Pt$ NMR spectroscopy in 0.1 mol dm$^{-3}$ HCl solutions at 298 K. The crystal structures of $(H_{10}[30]aneN_{10})[Pt(CN)_4]_5\cdot 2H_2O$ (**1**) and $(H_{10}[30]aneN_{10})(PtCl_6)_2Cl_6\cdot 2H_2O$ (**2**) solid compounds have been determined by X-ray analysis. In $(H_{10}[30]aneN_{10})[Pt(CN)_4]_5\cdot 2H_2O$ (space group $P\bar{1}$, $a$ = 12.710 (3) Å, $b$ = 9.839 (6) Å, $c$ = 11.630 (3) Å; $\alpha$ = 80.91 (4)°, $\beta$ = 89.45 (2)°, $\gamma$ = 77.60 (6)°; $V$ = 1402 (1) Å$^3$; $Z$ = 1; $R$ = 0.032; $R_w$ = 0.028) the centrosymmetric decaprotonated macrocycle has an elliptical shape with intramolecular distances between symmetry-related nitrogens of 6.2-13.4 Å. Two independent $Pt(CN)_4^{2-}$ anions, located outside the macrocyclic cavity, form very short hydrogen bonds with the protonated nitrogen atoms of the ligand. Also in $(H_{10}[30]aneN_{10})(PtCl_6)_2Cl_6\cdot 2H_2O$ (space group $P\bar{1}$, $a$ = 7.704 (9) Å, $b$ = 12.896 (4) Å, $c$ = 14.268 (10) Å; $\alpha$ = 108.87 (3)°, $\beta$ = 101.53 (7)°, $\gamma$ = 97.66 (5)°; $V$ = 1284 (2) Å$^3$; $Z$ = 1; $R$ = 0.058; $R_w$ = 0.048) the decacharged macrocyclic cation is centrosymmetric and presents an elliptical shape with intramolecular distances between symmetry-related nitrogen atoms of 9.6-11.4 Å. In the crystal packing there exists a wide network of intermolecular contacts involving the protonated nitrogen atoms of the macrocycle, $PtCl_6^{2-}$, $Cl^-$ anions, and water molecules. Both $PtCl_6^{2-}$ and $Cl^-$ anions are located outside the macrocyclic cavity. All results have been interpreted and discussed in terms of electrostatic attraction and hydrogen-bond formation between the polycharged macrocyclic cations and the complexed anions, as well as in terms of the mutual conformations of both species.

## Introduction

Macrocyclic polyammonium cations have shown to be good receptors for anionic complexed species.[2-8] In recent works we have found that polyammonium cations derived from polyazacycloalkanes of the series [3$k$]aneN$_k$ ($k$ = 7-12) form very stable second-sphere complexes (supercomplexes) with octahedral anions such as $Fe(CN)_6^{4-}$ and $Co(CN)_6^{3-}$.[4,5,8] The thermodynamic results presented revealed that the interaction between these anionic species and the macrocyclic receptors is mainly coulombic in nature. Furthermore the crystal structure of the solid compound $(H_8[30]aneN_{10})[Co(CN)_6]_2Cl_2\cdot 10H_2O$ evidenced the existence of a close hydrogen-bond network between the octacharged $(H_8[30]aneN_{10})^{8+}$ and $Co(CN)_6^{3-}$.[5] In this compound, the polyammonium cation, which presents an elliptical conformation, binds $Co(CN)_6^{3-}$ outside its macrocyclic cavity. This structure suggested that the conformation of the cyclic polycharged cation could produce a geometrical discrimination in anion binding, allowing, for instance, the inclusion of planar anionic species. Indeed we demonstrated that the planar $PdCl_4^{2-}$ can insert into the elongated cavity of $(H_{10}[30]aneN_{10})^{10+}$.[7] However, as shown by the crystal structure of $[(PdCl_4)(H_{10}[30]aneN_{10})](PdCl_4)_2Cl_4$, the $PdCl_4^{2-}$ anion is placed along the minor axis of the receptor's cavity, with the chlorine atoms standing out of the macrocyclic frame, thus forming strong hydrogen bonds with the polyammonium sites of the macrocycle.[7]

Therefore it seems that both the dimensions and conformation of the macrocycle as well as the geometry of the anion and an adequate mutual disposition are required to achieve an inclusive coordination. In this paper we report further investigations on the interaction of other planar $Pt(CN)_4^{2-}$ and octahedral $PtCl_6^{2-}$ complex anions with the polyammonium cations of the same series and we extend our study on the equilibria involving $Co(CN)_6^{3-}$ and $Fe(CN)_6^{4-}$ to all the terms of the series.

## Experimental Section

**Materials.** All potentiometric measurements were carried out in 0.15 mol dm$^{-3}$ $NaClO_4$ (C. Erba, ACS grade) purified accordingly to the procedure already described.[9] $K_4[Fe(CN)_6]\cdot 3H_2O$ (C. Erba, ACS grade) was used without further purification. $K_3[Co(CN)_6]$ (Aldrich, reagent grade) was recrystallized twice from an ethanol/water mixture. Samples of $K_2PtCl_6$ and $K_2Pt(CN)_4\cdot 3H_2O$, purchased from Aldrich, having purity greater than 99% were used without further purification. The hydrochloride salts of [3$k$]aneN$_k$ ($k$ = 7-12) ligands were obtained as previously reported.[10] Crystals of $(H_{10}[30]aneN_{10})[Pt(CN)_4]_5\cdot 2H_2O$ and $(H_{10}[30]aneN_{10})(PtCl_6)_2Cl_6\cdot 2H_2O$ were obtained by slow evaporation at room temperature of 1 mol dm$^{-3}$ HCl solutions (20 cm$^{-3}$) containing 0.1 mmol of [30]aneN$_{10}$ and 0.3 mmol of $K_2Pt(CN)_4\cdot 3H_2O$ and $K_2PtCl_6$, respectively. Satisfactory elemental analyses were obtained for both compounds.

**Emf Measurements.** The potentiometric titrations were carried out, in 0.15 mol dm$^{-3}$ $NaClO_4$ solutions at 298.15 K, by using the equipment (potentiometer, cell, burette, stirrer, microcomputer, etc.) that has previously been fully described.[11] The reference electrode was an Ag/AgCl electrode in saturated KCl solution. The glass electrode was calibrated

(1) (a) Department of Chemistry, University of Florence. (b) Department of Energetics, University of Florence. (c) University of Valencia. (d) University of Urbino.

(2) Peter, F.; Gross, M.; Hosseini, M. W.; Lehn, J. M.; Session, R. B. *J. Chem. Soc., Chem. Commun.* **1981**, 1067. Dietrich, B.; Hosseini, M. W.; Lehn, J. M.; Session, R. B. *J. Am. Chem. Soc.* **1981**, *103*, 1282. Peter, F.; Gross, M.; Hosseini, M. W.; Lehn, J. M. *J. Electroanal. Chem. Interfacial Electrochem.* **1983**, *144*, 279.

(3) Pina, F.; Moggi, L.; Manfrin, M. F.; Balzani, V.; Hosseini, M. W.; Lehn, J. M. *Gazz. Chim. Ital.* **1989**, *119*, 65.

(4) Garcia-España, E.; Micheloni, M.; Paoletti, P.; Bianchi, A. *Inorg. Chim. Acta* **1985**, *102*, L9.

(5) Bianchi, A.; Garcia-España, E.; Mangani, S.; Micheloni, M.; Orioli, P.; Paoletti, P. *J. Chem. Soc., Chem. Commun.* **1987**, 729. Bencini, A.; Bianchi, A.; Garcia-España, E.; Giusti, M.; Mangani, S.; Micheloni, M.; Orioli, P.; Paoletti, P. *Inorg. Chem.* **1987**, *26*, 3902.

(6) Bianchi, A.; Micheloni, M.; Orioli, P.; Paoletti, P.; Mangani, S. *Inorg. Chim. Acta* **1988**, *146*, 153.

(7) Bencini, A.; Bianchi, A.; Dapporto, P.; Garcia-España, E.; Micheloni, M.; Paoletti, P.; Paoli, P. *J. Chem. Soc., Chem. Commun.* **1990**, 753. Bencini, A.; Bianchi, A.; Micheloni, M.; Paoletti, P.; Dapporto, P.; Paoli, P.; Garcia-España, E. *J. Inclusion Phenom.* **1992**, *12*, 291.

(8) Aragó, J.; Bencini, A.; Bianchi, A.; Domenech, A.; Garcia-España, E. *J. Chem. Soc., Dalton Trans.* **1992**, 319.

(9) Micheloni, M.; May, P. M.; Williams, D. R. *J. Inorg. Nucl. Chem.* **1978**, *40*, 1209.

(10) Micheloni, M.; Paoletti, P.; Bianchi, A. *Inorg. Chem.* **1985**, *24*, 3702. Bianchi, A.; Mangani, S.; Micheloni, M.; Nanini, V.; Orioli, P.; Paoletti, P.; Seghi, B. *Inorg. Chem.* **1984**, *23*, 1182. Bencini, A.; Bianchi, A.; Garcia-España, E.; Giusti, M.; Micheloni, M.; Paoletti, P. *Inorg. Chem.* **1987**, *26*, 681. Bencini, A.; Bianchi, A.; Garcia-España, E.; Giusti, M.; Mangani, S.; Micheloni, M.; Orioli, P.; Paoletti, P. *Inorg. Chem.* **1987**, *26*, 1243. Bencini, A.; Bianchi, A.; Garcia-España, E.; Micheloni, M.; Paoletti, P. *Inorg. Chem.* **1988**, *27*, 176.

(11) Bianchi, A.; Bologni, L.; Dapporto, P.; Micheloni, M.; Paoletti, P. *Inorg. Chem.* **1984**, *13*, 1201.

0020-1669/92/1331-1902$03.00/0 

**Table I.** Crystal and Refinement Data for $(H_{10}[30]aneN_{10})[Pt(CN)_4]_5\cdot 2H_2O$ and for $(H_{10}[30]aneN_{10})(PtCl_6)_2Cl_6\cdot 2H_2O$

| | | |
|---|---|---|
| mol formula | $C_{40}H_{64}N_{30}O_2Pt_5$ | $C_{20}H_{64}Cl_{18}N_{10}O_2Pt_2$ |
| mol wt | 1972.55 | 1505.11 |
| cryst dimens, mm | 0.1 × 0.2 × 0.5 | 0.2 × 0.5 × 0.6 |
| $a$, Å | 12.710 (3) | 7.704 (9) |
| $b$, Å | 9.839 (6) | 12.896 (4) |
| $c$, Å | 11.630 (3) | 14.268 (10) |
| $\alpha$, deg | 80.91 (4) | 108.87 (3) |
| $\beta$, deg | 89.45 (2) | 101.53 (7) |
| $\gamma$, deg | 77.60 (6) | 97.66 (5) |
| $V$, Å$^3$ | 1402 (1) | 1284 (2) |
| $Z$ | 1 | 1 |
| space group | $P\bar{1}$ | $P\bar{1}$ |
| $D_c$, g cm$^{-3}$ | 2.34 | 1.95 |
| radiation | graphite monochromated Mo–K$\alpha$ ($\lambda$ = 0.7107 Å) | |
| temp, K | 298 | 298 |
| $\mu$, cm$^{-1}$ | 120.1 | 64.8 |
| range of transm factors | 0.09–0.30 | 0.14–0.29 |
| $R^a$ | 0.032 | 0.058 |
| $R_w^b$ | 0.028 | 0.048 |

$^a R = \sum||F_o| - |F_c||/\sum|F_o|$. $^b R_w = [\sum w(|F_o| - |F_c|)^2/\sum w(F_o)^2]^{1/2}$.

as a hydrogen concentration probe by titration of well-known amounts of HCl with $CO_2$-free NaOH solutions and determining the equivalent point by the Gran method,[12] which gives the standard potential $E°$, and the ionic product of water. The computer program SUPERQUAD[13] was used to calculate the equilibrium constants. The titration curves for each system were treated either as a single set or as separated curves without significant variations in the values of the equilibrium constants. Furthermore, the sets of data were merged together and treated simultaneously to give the final equilibrium constants. To avoid protonation of the $Fe(CN)_6^{4-}$ anion, all experiments were carried out at a pH higher than 3.5. Protonation of the other anions does not take place over the pH range (2.5–11) investigated, as proved by potentiometric titration.

**Spectroscopy.** The 43.00-MHz $^{195}$Pt NMR spectra were recorded at 298 K in a Bruker AC-200 spectrometer. All samples were prepared in 0.1 mol dm$^{-3}$ HCl. Chemical shifts are referred to solvated $PtCl_6^{2-}$ and $Pt(CN)_4^{2-}$ under the same experimental conditions. Addition of an excess of chloride anion does not affect the chemical shift of the free anions.

**Collection and Reduction of X-ray Intensity Data.** A pale yellow prismatic crystal of $(H_{10}[30]aneN_{10})[Pt(CN)_4]_5\cdot 2H_2O$ (**1**) and a yellow prismatic crystal of $(H_{10}[30]aneN_{10})(PtCl_6)_2Cl_6\cdot 2H_2O$ (**2**) were epoxied to glass fibers and mounted on an Enraf-Nonius CAD4 automatic diffractometer, which uses the equatorial diffraction geometry. A summary of crystallographic data is reported in Table I. Unit cell parameters of both compounds were determined by least-squares refinement of diffractometer setting angles of 25 carefully centered reflections. During data collections, three reflections were monitored periodically to check for the stability of the diffractometer and of the crystals: no loss of intensity was noticed during data collections. Intensities were corrected for Lorentz and polarization effects; an absorption correction was applied, once the structures were solved, by using the Walker and Stuart method.[14] No extinction correction was applied.

**$(H_{10}[30]aneN_{10})[Pt(CN)_4]_5\cdot 2H_2O$.** A total of 3916 unique reflections ($5 \le 2\theta \le 45°$, Mo K$\alpha$ radiation) were collected of which 3341 having $I > 3\sigma(I)$ were used in the structure solution and refinement. The structure was solved by the heavy-atom technique, which showed the platinum atoms. Subsequent Fourier maps showed all non-hydrogen atoms. Refinement was performed by means of the full-matrix least-squares method. Hydrogen atoms, except those of the water molecule, were included in calculated positions with an overall temperature factor $U$ of 0.05 Å$^2$. Anisotropic thermal parameters were used for all the non-hydrogen atoms. The final atomic coordinates for non-hydrogen atoms are listed in Table II.

**$(H_{10}[30]aneN_{10})(PtCl_6)_2Cl_6\cdot 2H_2O$.** A total of 4223 unique reflections ($5 \le 2\theta \le 50°$, Mo K$\alpha$ radiation) were collected of which 3225 having $I > 3\sigma(I)$ were used in the structure analysis. The structure was solved by the heavy-atom technique, with the use of a Patterson map, which showed the position of the platinum atom. Subsequent $F_o$ and $\Delta F$ Fourier syntheses showed the positions of all non-hydrogen atoms; the hydrogen atoms, except those of the water molecule, were included in calculated positions. Refinement was performed by means of the full-matrix least-squares method. Anisotropic thermal parameters were used for all the non-hydrogen atoms. The final atomic coordinates for all the non-

**Table II.** Positional Parameters (×10$^4$) with their Esds in Parentheses for $(H_{10}[30]aneN_{10})[Pt(CN)_4]_5\cdot 2H_2O$

| atom | $x/a$ | $y/b$ | $z/c$ |
|---|---|---|---|
| Pt1 | 0 | -5000 | 0 |
| N11 | 488 (8) | -2622 (10) | 1313 (9) |
| C11 | 328 (9) | -3480 (12) | 793 (10) |
| N12 | 1870 (8) | -4766 (10) | -1757 (8) |
| C12 | 1171 (9) | -4824 (10) | -1137 (10) |
| Pt2 | 8331 (1) | -2629 (1) | 8008 (1) |
| N21 | 6859 (8) | -4734 (10) | 8839 (9) |
| C21 | 7381 (10) | -3972 (12) | 8538 (10) |
| N22 | 7316 (8) | -913 (11) | 9959 (9) |
| C22 | 7647 (10) | -1519 (12) | 9215 (10) |
| N23 | 9452 (8) | -4555 (10) | 6223 (9) |
| C23 | 9061 (11) | -3832 (14) | 6872 (13) |
| N24 | 9717 (8) | -342 (10) | 7314 (9) |
| C24 | 9244 (10) | -1200 (12) | 7555 (10) |
| Pt3 | 5724 (1) | -1546 (1) | 6160 (1) |
| N31 | 4176 (9) | -3431 (10) | 7237 (9) |
| C31 | 4738 (9) | -2768 (12) | 6837 (11) |
| N32 | 4627 (9) | 542 (12) | 7819 (10) |
| C32 | 5062 (10) | -210 (13) | 7206 (11) |
| N33 | 6580 (8) | -3799 (10) | 4543 (9) |
| C33 | 6310 (11) | -2938 (13) | 5124 (10) |
| C34 | 6675 (10) | -245 (12) | 5462 (10) |
| N34 | 7200 (8) | 494 (9) | 5086 (9) |
| N1 | -1563 (7) | -712 (9) | 1928 (8) |
| C1 | -1709 (9) | -1855 (12) | 2865 (10) |
| C2 | -1100 (8) | -1867 (12) | 3983 (10) |
| N2 | 85 (7) | -2516 (9) | 3928 (8) |
| C3 | 697 (9) | -2204 (11) | 4923 (10) |
| C4 | 1625 (8) | -3413 (11) | 5405 (10) |
| N3 | 2684 (7) | -3312 (9) | 4914 (7) |
| C5 | 2771 (9) | -3298 (12) | 3643 (9) |
| C6 | 3966 (9) | -3256 (12) | 3319 (10) |
| N4 | 4153 (7) | -3413 (8) | 2094 (7) |
| C7 | 3578 (9) | -2242 (11) | 1226 (10) |
| C8 | 3895 (9) | -2397 (12) | -19 (10) |
| N5 | 3056 (7) | -2868 (9) | -668 (8) |
| C9 | 2070 (10) | -1754 (12) | -993 (10) |
| C10 | 2266 (9) | -701 (11) | -2012 (10) |
| O1 | 6133 (6) | -3277 (9) | 1444 (8) |

**Table III.** Positional Parameters (×10$^4$) with their Esds in Parentheses for $(H_{10}[30]aneN_{10})(PtCl_6)_2Cl_6\cdot 2H_2O$

| atom | $x/a$ | $y/b$ | $z/c$ |
|---|---|---|---|
| Pt1 | 6465 (1) | 4440 (1) | -2585 (1) |
| Cl1 | 5425 (6) | 2499 (3) | -3284 (3) |
| Cl2 | 7396 (6) | 6369 (3) | -1918 (4) |
| Cl3 | 8481 (7) | 4282 (4) | -3593 (4) |
| Cl4 | 4255 (8) | 4575 (4) | -3880 (4) |
| Cl5 | 4435 (8) | 4582 (4) | -1587 (5) |
| Cl6 | 8654 (7) | 4313 (4) | -1298 (4) |
| C1 | 7592 (23) | 3169 (13) | 980 (13) |
| N1 | 6816 (16) | 1933 (9) | 223 (9) |
| C2 | 5858 (20) | 1893 (13) | -838 (11) |
| C3 | 4111 (20) | 2258 (12) | -781 (11) |
| N2 | 2969 (16) | 1831 (10) | -1867 (10) |
| C4 | 1161 (20) | 2197 (13) | -1954 (12) |
| C5 | 28 (20) | 1790 (13) | -3046 (12) |
| N3 | -795 (16) | 570 (10) | -3491 (9) |
| C6 | -2426 (19) | 218 (12) | -3152 (12) |
| C7 | -3087 (21) | -1003 (13) | -3747 (12) |
| N4 | -4719 (17) | -1374 (9) | -3429 (9) |
| C8 | -5609 (17) | -2637 (12) | -3932 (11) |
| C9 | -7223 (22) | -2926 (13) | -3589 (11) |
| N5 | -6611 (18) | -3033 (10) | -2553 (10) |
| C10 | -8217 (23) | -3235 (13) | -2084 (12) |
| C17 | -3677 (6) | -879 (3) | -1084 (3) |
| C18 | -2581 (6) | 152 (3) | 4256 (3) |
| C19 | -1388 (7) | 510 (3) | 1966 (3) |
| O1 | -28 (14) | 1290 (8) | -151 (8) |

(12) Gran, G. *Analyst (London)* **1952**, *77*, 661. Rossotti, F. J.; Rossotti, H. *J. Chem. Educ.* **1989**, *28*, 1188.
(13) Gans, P.; Sabatini, A.; Vacca, A. *J. Chem. Soc., Dalton Trans.* **1985**, 1195.
(14) Walker, N.; Stuart, D. D. *Acta Crystallogr., Sect. A* **1983**, *A39*, 158.

**Table IV.** Dihedral Angles (deg) for the Macrocyclic Ligands

| | | | |
|---|---|---|---|
| | $(H_{10}[30]aneN_{10})[Pt(CN)_4]_5 \cdot 2H_2O$ | | |
| N1-C1-C2-N2 | -78 (1) | C6-N4-C7-C8 | 174 (1) |
| C1-C2-N2-C3 | 167 (1) | N4-C7-C8-N5 | 103 (1) |
| C2-N2-C3-C4 | 144 (1) | C7-C8-N5-C9 | 73 (1) |
| N2-C3-C4-N3 | 95 (1) | C8-N5-C9-C10 | 76 (1) |
| C3-C4-N3-C5 | -61 (1) | N5-C9-C10-N1′ | -150 (1) |
| C4-N3-C5-C6 | -177 (1) | C1-N1-C10′-C9′ | -178 (1) |
| N3-C5-C6-N4 | 173 (1) | C10′-N1-C1-C2 | -81 (1) |
| C5-C6-N4-C7 | 67 (1) | | |
| | $(H_{10}[30]aneN_{10})(PtCl_6)_2Cl_6 \cdot 2H_2O$ | | |
| N1-C1-C10′-N5′ | -74 (2) | C5-N3-C6-C7 | 176 (1) |
| C10′-C1-N1-C2 | 169 (1) | N3-C6-C7-N4 | -180 (1) |
| C1-N1-C2-C3 | -72 (1) | C6-C7-N4-C8 | -178 (1) |
| N1-C2-C3-N2 | -161 (1) | C7-N4-C8-C9 | -179 (1) |
| C2-C3-N2-C4 | -176 (1) | N4-C8-C9-N5 | -81 (1) |
| C3-N2-C4-C5 | 179 (1) | C8-C9-N5-C10 | 175 (1) |
| N2-C4-C5-N3 | 73 (2) | C9-N5-C10-C1′ | -171 (1) |
| C4-C5-N3-C6 | 77 (2) | | |

hydrogen atoms are reported in Table III. Table IV reports the macrocycle torsion angles for both structures.

All calculations were performed on an IBM PS/2 80 computer with the SHELX-76 set of programs[15] that use the analytical approximation for the atomic scattering factors and anomalous dispersion corrections for all atoms from ref 16. The molecular plots were produced by the program ORTEP.[17]

## Results and Discussion

**Description of the Structures.** The molecular structure of $(H_{10}[30]aneN_{10})[Pt(CN)_4]_5 \cdot 2H_2O$ consists of the $[C_{20}H_{60}N_{10}]^{10+}$ cation (L1), complex $Pt(CN)_4^{2-}$ anions, and water molecules. The fully protonated macrocycle is centrosymmetric, as is the $Pt(CN)_4^{2-}$ anion containing the Pt1 atom (Figure 1). The other two independent $Pt(CN)_4^{2-}$ anions are in general positions. The decaprotonated macrocycle has an elongated elliptical shape (Figure 2f) with the intramolecular distances between symmetry-related nitrogen atoms being between 6.2 and 13.4 Å. In order to evaluate the relative arrangement of the nitrogen donor atoms the mean square plane through them has been evaluated: the N5 atom (Figure 1) exhibits a large deviation (1.091 (9) Å) from this plane. The most remarkable feature of this structure is the presence of an array of short hydrogen bonds between all protonated nitrogens of the macrocycle and the two independent $Pt(CN)_4^{2-}$ anions whose nitrogen atoms directly point toward the macrocyclic framework (Figure 3). Furthermore an additional hydrogen bond is established between the protonated nitrogen atom N4 and the oxygen atom of the water molecule (O1···HO41, 1.60 (1) Å).

The crystal structure of $(H_{10}[30]aneN_{10})(PtCl_6)_2Cl_6 \cdot 2H_2O$ consists of $[C_{20}H_{60}N_{10}]^{10+}$ (L2) centrosymmetric cations, $PtCl_6^{2-}$ anions, chloride anions, and water molecules (Figure 4). In the crystal packing there exists a wide network of intermolecular contacts involving the hydrogens of the protonated nitrogen atoms, the $PtCl_6^{2-}$ anions, the chlorine atoms, and the oxygen atom of the water molecule (Figure 5). Particularly the chloride ion Cl7 is situated over the ligand cavity because of an interaction via hydrogen bonds with three adjacent nitrogen atoms of the macrocycle: the Cl7 anion is located 1.21 Å above the plane defined by N1, N4 and N5. All of the protons involved in this short contact point inside the macrocyclic cavity. This arrangement of the bridging hydrogen atoms is achieved by a gauche conformation of the dihedral angles N1-C1-C10′-N5′ and N4-C8-C9-N5 (Figure 4, Table IV), -74 (2) and -81 (1)°, respectively. Also in this case the macrocycle is centrosymmetric. The overall resulting shape of the macrocycle (Figure 2h,i) is less elongated (9.6-11.4 Å) than that of L1 with comparable deviations of the nitrogen atoms from the mean square plane, with the N1 atoms having the largest deviation (0.89 (1) Å).

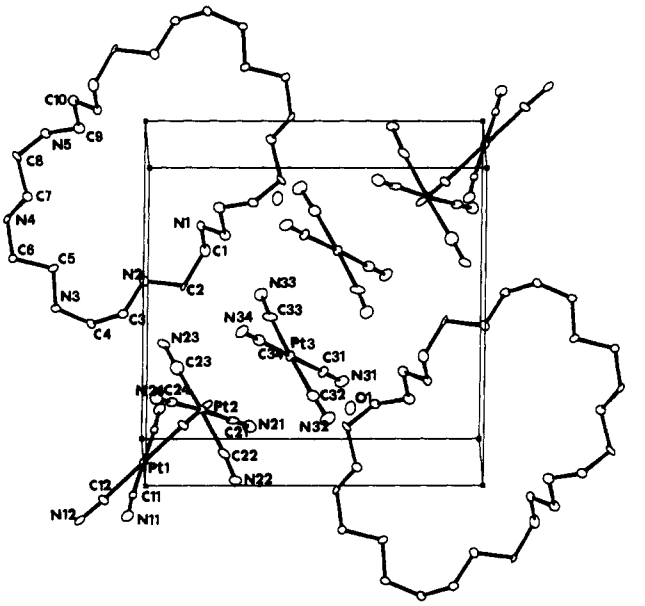


**Figure 1.** ORTEP drawing of the crystal packing of $(H_{10}[30]aneN_{10})[Pt(CN)_4]_5 \cdot 2H_2O$.

**Solution Equilibria.** The coordinating ability of the polyammonium cations derived from the macrocycles of the series $[3k]aneN_k$ ($k$ = 7-12) toward $Fe(CN)_6^{4-}$ and $Co(CN)_6^{3-}$ is shown in Figure 6 where the logarithms of the equilibrium constants (Tables V and VI) for the formation of the supercomplexed species, at each protonation degree, have been plotted versus the number of nitrogen atoms present in the macrocyclic receptors. For all the systems studied only 1:1 anion-receptor species are formed, whose stability increases with the degree of protonation of the macrocycle. The formation of these species can be detected when the cyclic polyamines are at least tetracharged. Only in the case of $[21]aneN_7$, the smallest among the ligands here considered, has the interaction with the tricharged form also been observed, while for the largest, $[36]aneN_{12}$, at least the pentaprotonated form is required for the interaction with $Fe(CN)_6^{4-}$ to be detected. These features indicates that electrostatic interaction plays a major role in the strength of anion binding. Furthermore, as can be seen for $Fe(CN)_6^{4-}$, the stability of the supercomplexed species, at each degree of protonation, decreases accordingly with the increasing dimensions of the macrocycles with a greater dispersion of the positive charges. However, in the case of $Co(CN)_6^{3-}$ an inversion of this trend has been observed from $[30]aneN_{10}$ to $[33]aneN_{11}$.[5] This phenomenon was interpreted by Pina et al.[3] on the base of the quantum yield of the photoaquation reaction of the bound $Co(CN)_6^{3-}$, by assuming the inclusion of the tricharged anion into the cavity of the polyprotonated $[33]aneN_{11}$. For $[36]aneN_{12}$ different behaviors are observed for two different groups of protonated species. The tetra-, penta-, and hexaprotonated forms of $[36]aneN_{12}$ produce with $Co(CN)_6^{3-}$ supercomplexes whose stability is greater than that presented by the analogous species of $[33]aneN_{11}$, while the forms with higher degree of protonation (7-10) present lower stability. These opposite tendencies give rise to a close grouping of the equilibrium constants. A similar, even if less marked, grouping is also observed for the supercomplexed species of $[36]aneN_{12}$ with $Fe(CN)_6^{4-}$.

In the case of the dicharged anion $Pt(CN)_4^{2-}$ the supercomplexed species formed with the protonated forms of the macrocyclic receptors from $[21]aneN_7$ to $[30]aneN_{10}$ present a lower stability (Table VII) than the analogous species with $Fe(CN)_6^{4-}$ and $Co(CN)_6^{3-}$, respectively. Furthermore a lower gain in stability is observed for each one of these macrocycles as the degree of protonation increases, and for a given degree of protonation the stability of the supercomplexes is less influenced by the dimension of the macrocycle (Figure 7). On the other hand, a noticeable increase of the stability of the $Pt(CN)_4^{2-}$ anion complexes is

(15) Sheldrick, G. M. *SHELX-76*, Program for Crystal Structure Determination; University of Cambridge: Cambridge, England, 1976.
(16) *International Tables for X-ray Crystallography*; Kynoch: Birmingham, England, 1974; Vol. IV.
(17) Johnson, C. K. ORTEP. Report ORNL-3794; Oak Ridge National Laboratory: Oak Ridge, TN, 1971.

**Table V.** Logarithms of the Equilibrium Constants for the Formation of the Anion Complexes of the Protonated Species of $[3k]aneN_k$ ($k$ = 7–12) Polyazacycloalkanes with $Co(CN)_6^{3-}$ in 0.15 mol $dm^{-3}$ $NaClO_4$ at 25 °C

| | log $K$ | | | | | |
|---|---|---|---|---|---|---|
| reaction | [21]aneN$_7$[a] | [24]aneN$_8$[a] | [27]aneN$_9$[b] | [30]aneN$_{10}$[b] | [33]aneN$_{11}$[b] | [36]aneN$_{12}$[c] |
| $LH_3^{3+} + Co(CN)_6^{3-} = LH_3Co(CN)_6$ | 2.7 | | | | | |
| $LH_4^{4+} + Co(CN)_6^{3-} = [LH_4Co(CN)_6]^+$ | 3.5 | 2.9 | 2.61 | 2.03 | 2.63 | 3.22 (5)[d] |
| $LH_5^{5+} + Co(CN)_6^{3-} = [LH_5Co(CN)_6]^{2+}$ | 3.7 | 3.5 | 3.00 | 2.10 | 3.05 | 3.61 (5) |
| $LH_6^{6+} + Co(CN)_6^{3-} = [LH_6Co(CN)_6]^{3+}$ | 4.2 | 3.9 | 3.36 | 2.37 | 3.52 | 3.83 (4) |
| $LH_7^{7+} + Co(CN)_6^{3-} = [LH_7Co(CN)_6]^{4+}$ | 4.8 | 4.1 | 3.78 | 3.23 | 4.05 | 3.92 (7) |
| $LH_8^{8+} + Co(CN)_6^{3-} = [LH_8Co(CN)_6]^{5+}$ | | | 4.09 | 3.66 | 4.55 | 4.20 (7) |
| $LH_9^{9+} + Co(CN)_6^{3-} = [LH_9Co(CN)_6]^{6+}$ | | | | 4.43 | 4.87 | 4.44 (7) |
| $LH_{10}^{10+} + Co(CN)_6^{3-} = [LH_{10}Co(CN)_6]^{7+}$ | | | | | 5.32 | 4.44 (9) |
| $LH_{11}^{11+} + Co(CN)_6^{3-} = [LH_{11}Co(CN)_6]^{8+}$ | | | | | | 5.10 (6) |

[a] From ref 8. [b] From ref 5. [c] This work. [d] Values in parentheses are standard deviations in the last significant figure.

**Table VI.** Logarithms of the Equilibrium Constants for the Formation of the Anion Complexes of the Protonated Species of $[3k]aneN_k$ ($k$ = 7–12) Polyazacycloalkanes with $Fe(CN)_6^{4-}$ in 0.15 mol $dm^{-3}$ $NaClO_4$ at 25 °C

| | log $K$ | | | | | |
|---|---|---|---|---|---|---|
| reaction | [21]aneN$_7$[a] | [24]aneN$_8$[a] | [27]aneN$_9$[b] | [30]aneN$_{10}$[b] | [33]aneN$_{11}$[b] | [36]aneN$_{12}$[c] |
| $LH_3^{3+} + Fe(CN)_6^{4-} = [LH_3Fe(CN)_6]^-$ | 3.4 | | | | | |
| $LH_4^{4+} + Fe(CN)_6^{4-} = LH_4Fe(CN)_6$ | 5.1 | 4.1 | 4.06 | 3.69 | 3.61 | |
| $LH_5^{5+} + Fe(CN)_6^{4-} = [LH_5Fe(CN)_6]^+$ | 6.6 | 5.5 | 5.63 | 4.78 | 4.66 | 4.57 (2)[d] |
| $LH_6^{6+} + Fe(CN)_6^{4-} = [LH_6Fe(CN)_6]^{2+}$ | | 7.1 | 7.60 | 6.23 | 5.72 | 5.16 (2) |
| $LH_7^{7+} + Fe(CN)_6^{4-} = [LH_7Fe(CN)_6]^{3+}$ | | | 9.33 | 7.92 | 6.93 | 5.96 (5) |
| $LH_8^{8+} = Fe(CN)_6^{4-} = [LH_8Fe(CN)_6]^{4+}$ | | | | 9.03 | 8.07 | 6.96 (5) |
| $LH_9^{9+} + Fe(CN)_6^{4-} = [LH_9Fe(CN)_6]^{5+}$ | | | | | | 7.53 (6) |

[a] From ref 8. [b] From ref 5. [c] This work. [d] Values in parentheses are standard deviations in the last significant figure.

**Table VII.** Logarithms of the Equilibrium Constants for the Formation of the Anion complexes of the Protonated Species of $[3k]aneN_k$ ($k$ = 7–11) Polyazacycloalkanes with $Pt(CN)_4^{2-}$ in 0.15 mol $dm^{-3}$ $NaClO_4$ at 25 °C

| | log $K$ | | | | |
|---|---|---|---|---|---|
| reaction | [21]aneN$_7$ | [24]aneN$_8$ | [27]aneN$_9$ | [30]aneN$_{10}$ | [33]aneN$_{11}$ |
| $LH_3^{3+} + Pt(CN)_4^{2-} = [LH_3Pt(CN)_4]^+$ | 2.56 (2)[a] | 2.48 (6) | | | |
| $LH_4^{4+} + Pt(CN)_4^{2-} = [LH_4Pt(CN)_4]^{2+}$ | 3.07 (2) | 3.00 (3) | 3.00 (2) | 2.69 (3) | 3.17 (5) |
| $LH_5^{5+} + Pt(CN)_4^{2-} = [LH_5Pt(CN)_4]^{3+}$ | 3.49 (2) | 3.44 (4) | 3.53 (2) | 2.77 (3) | 3.60 (2) |
| $LH_6^{6+} + Pt(CN)_4^{2-} = [LH_6Pt(CN)_4]^{4+}$ | 3.61 (3) | 3.53 (4) | 3.80 (2) | 3.14 (4) | 4.71 (4) |
| $LH_7^{7+} + Pt(CN)_4^{2-} = [LH_7Pt(CN)_4]^{5+}$ | 3.71 (7) | 3.59 (5) | 3.83 (2) | 3.36 (3) | 5.46 (4) |
| $LH_8^{8+} + Pt(CN)_4^{2-} = [LH_8Pt(CN)_4]^{6+}$ | | 3.71 (7) | 4.17 (3) | 3.44 (4) | 5.83 (4) |
| $LH_9^{9+} + Pt(CN)_4^{2-} = [LH_9Pt(CN)_4]^{7+}$ | | | | 3.83 (4) | 6.09 (5) |
| $LH_{10}^{10+} + Pt(CN)_4^{2-} = [LH_{10}Pt(CN)_4]^{8+}$ | | | | | 6.67 (4) |

[a] Values in parentheses are standard deviations in the last significant figure.

observed from [30]aneN$_{10}$ to [33]aneN$_{11}$ (Figure 7). As previously reported,[5] a similar increase was observed for the analogous supercomplexes of $Co(CN)_6^{3-}$ and attributed to the inclusion of the anion into the receptor's cavity.[8] This increase is so large that $Pt(CN)_4^{2-}$ interacts with the protonated species of [33]aneN$_{11}$ stronger than the more charged $Co(CN)_6^{3-}$ (Tables V and VII).

As previously observed,[5] for similar systems in which many species are formed whose formation constants differ very slightly, great care has to be taken in the species selection criteria. Independent techniques to determine both the stoichiometry and the stability constants of the species formed are advisable. In the case of the $Fe(CN)_6^{4-}$ complexes electrochemical measurements were carried out at different macrocycle:anion molar ratios and at various pH's, and the results obtained were in good agreement with those obtained from potentiometry, confirming the 1:1 monomeric nature of the supercomplexed species formed.[5,8] In the case of $Pt(CN)_4^{2-}$ the variation of the $^{195}Pt$ NMR chemical shift with the $(H_k[3k]aneN_k)^{k+}$:anion molar ratio ($R$) has been followed. At $R > 1$, the interaction of $Pt(CN)_4^{2-}$ with the polyammonium $(H_k[3k]aneN_k)^{k+}$ receptors produces a constant upfield shift of the $^{195}Pt$ NMR signal of about 30 ppm with respect to the free anion, which could account for the formation of stable 1:1 supercomplexed species. Unfortunately at $R < 1$, under the experimental conditions employed, precipitation of polyammonium salts of $Pt(CN)_4^{2-}$ occurs, preventing then the investigation of whether the formation of polynucleated species in solution takes place or not.

The interaction of the octahedral anion $PtCl_6^{2-}$ with the polyammonium cations derived for $[3k]aneN_k$ ligands ($k$ = 7–11) can be studied only in very acidic solutions in order to prevent the formation of platinum(IV) macrocyclic complexes. Therefore the equilibria of supercomplex formation at various pH could not be studied, and only the interaction of this anion with the fully protonated $(H_k[3k]aneN_k)^{k+}$ species has been followed by $^{195}Pt$ NMR spectroscopy in 0.1 mol $dm^{-3}$ HCl solution. In all cases the presence of the polycharged macrocyclic receptors caused an upfield shift of the $^{195}Pt$ NMR signal with respect to the chemical shift of the solvated $PtCl_6^{2-}$. The upfield shift accordingly increases with the receptor:$PtCl_6^{2-}$ molar ratio with an increasing fraction of complexed $PtCl_6^{2-}$. As shown in Figure 8 for $(H_{10}[30]aneN_{10})^{10+}$ the chemical shift reaches a constant value for $R > 1$. Apart from the main inflection observed at $R = 1$, due to the formation of 1:1 supercomplexed species, a less evident inflection is present at $R$ values of about 0.5, which can be ascribed to the interaction of two $PtCl_6^{2-}$ anions with one macrocyclic molecule. Similar plots have been obtained for all the polyammonium receptors here considered.

## Conclusion

If the thermodynamic (Tables V–VII) and structural data up to now available for the interaction of di-, tri-, and tetracharged complex anions with the series of polyammonium receptors deriving from $[3k]aneN_k$ macrocycles are reviewed, a few features can be highlighted.

**(i) Coulombic Contribution.** Cation–anion electrostatic attraction is the driving force in supercomplexation reactions. Coulombic interaction appears as the main contribution to the stability of these new species, regulating the stability order of

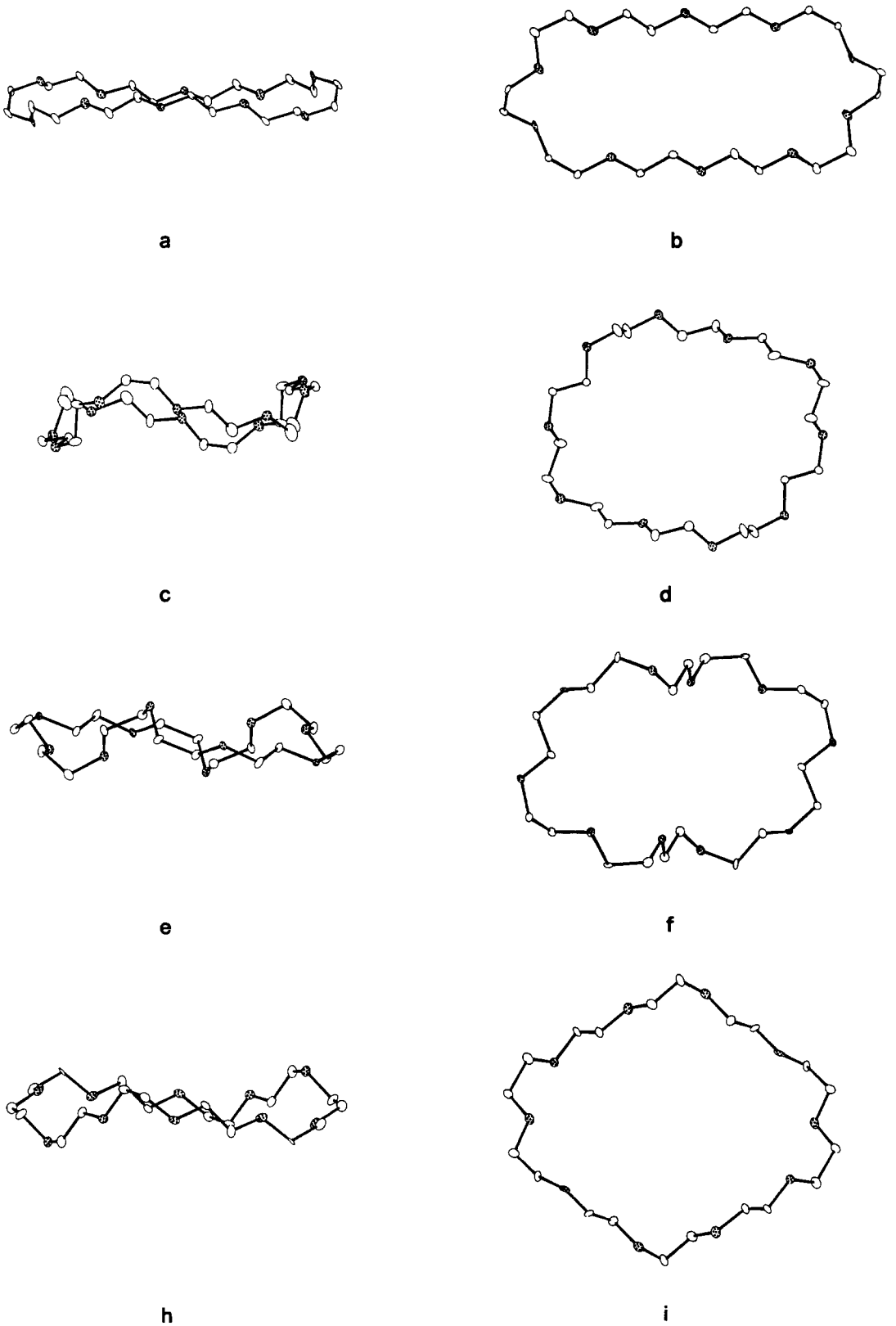


**Figure 2.** Lateral (left side) and top (right side) views of the $(H_8[30]aneN_{10})^{8+}$ cation in $(H_8[30]aneN_{10})[Co(CN)_6]_2Cl_2 \cdot 10H_2O$ (a, b) and of $(H_{10}[30]aneN_{10})^{10+}$ in $[(PdCl_4)(H_{10}[30]aneN_{10})](PdCl_4)_2Cl_4$ (c, d), $(H_{10}[30]aneN_{10})[Pt(CN)_4]_5 \cdot 2H_2O$ (e, f), and $(H_{10}[30]aneN_{10})(PtCl_6)_2Cl_6 \cdot 2H_2O$ (h, i). Dotted atoms are nitrogens.

supercomplexes with di-, tri-, and tetracharged anions ($Pt(CN)_4^{2-}$ < $Co(CN)_6^{3-}$ < $Fe(CN)_6^{4-}$) as well as with differently protonated receptors. Furthermore, it seems that electrostatic forces also contribute to regulate the stoichiometry of the species formed. In fact formation of 1:2 receptor–anion species have been observed for low-charged anions ($PdCl_4^{2-}$, $PtCl_6^{2-}$), i.e., for highly charged 1:1 complexes.

The few exceptions to the above trends can be ascribed to a particular matching between the conformational features of both receptor and anion which optimizes electrostatic and H-bond interactions.

**(ii) H-Bonding Contribution.** As previously observed,[5,7] also the crystal structures of the supercomplexed species here reported are characterized by the presence of extensive hydrogen-bond

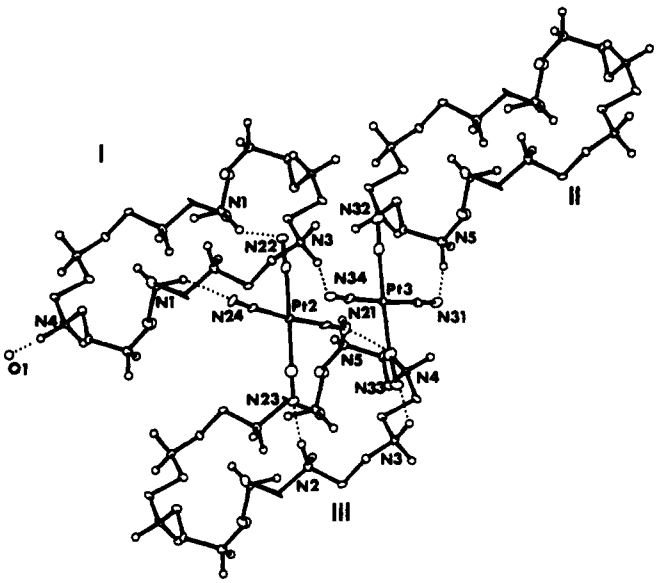


**Figure 3.** ORTEP drawing showing the intermolecular hydrogen bonds (<2.2 Å) in $(H_{10}[30]aneN_{10})[Pt(CN)_4]_5 \cdot 2H_2O$. Symmetry codes relating the macrocyclic molecules with respect to the $[Pt(CN)_4]^{2-}$ anions are as follows: (I) $-x + 1, -y, -z + 1$; (II) $x, y, z + 1$; (III) $-x + 1, -y - 1, -z + 1$. Interatomic distances are as follows: (Å) N21···HO42, 1.80 (1); N21···HO51, 1.92 (1); N22···HO12, 1.78 (1); N23···HO21, 1.79 (1); N31···HO52, 1.82 (1); N33···HO32, 1.91 (1); N34···HO31, 1.79 (1); O1···HO41, 1.60 (1). Only the hydrogen atoms of the ammonium groups are shown.

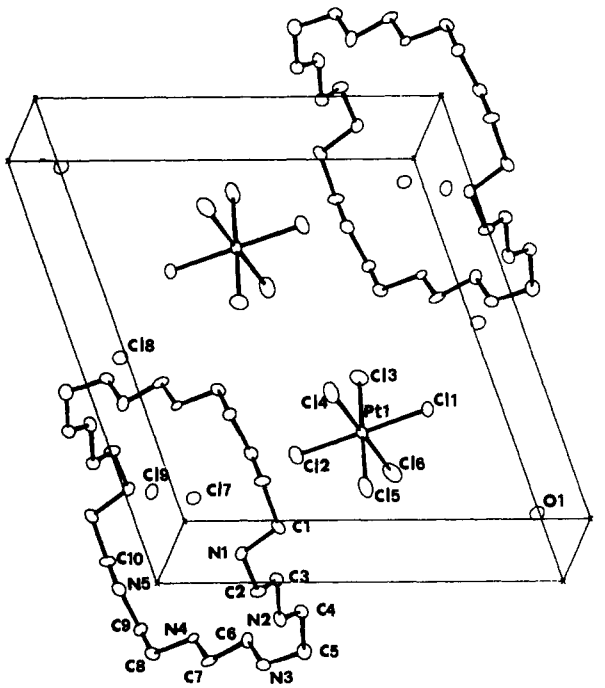


**Figure 4.** ORTEP drawing of the crystal packing of $(H_{10}[30]aneN_{10})(PtCl_6)_2Cl_6 \cdot 2H_2O$.

networks involving macrocyclic polyammonium cations, complexed anions, other anionic species, and water molecules. Of course the pictures offered by these structures, in the solid state, are not reliable representations of the receptor–anion specific interaction in solution. However these structures visualize, to some extent, the short contacts, between the macrocyclic receptor and the complexed anions, which must exist also in solution on account of the high values of the formation constants determined for the resulting species.

The formation of a supercomplex in solution partially disrupts the hydrogen-bonding to the solvent of both receptors and anion and creates, between these two species, new hydrogen bonds. The

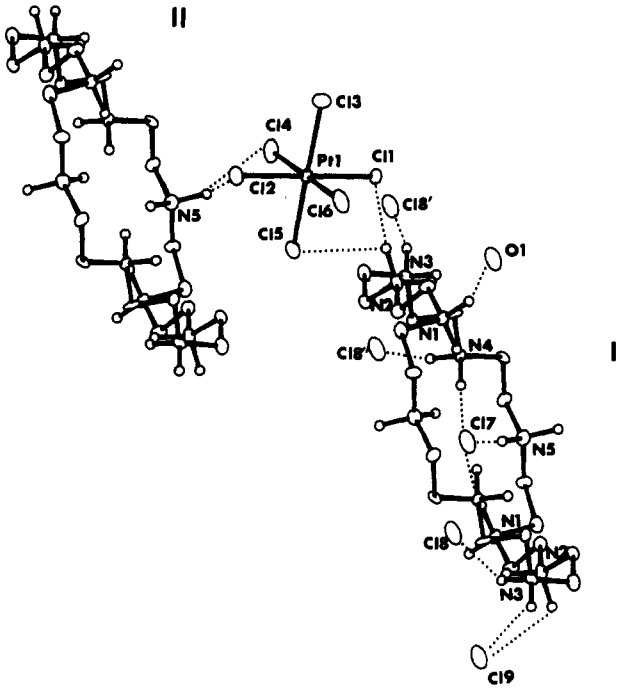


**Figure 5.** ORTEP drawing showing the intermolecular hydrogen bonds (<3 Å) in $(H_{10}[30]aneN_{10})(PtCl_6)_2Cl_6 \cdot 2H_2O$. Symmetry codes relating the macrocyclic molecules with respect to the $(PtCl_6)^{2-}$ anions are as follows: (I) $x, y, z$; (II) $x - 1, y - 1, z$. Interatomic distances (Å) are as follows: Cl1···HO22, 2.19 (2); Cl5···HO22, 2.92 (1); Cl2···HO52, 2.52 (1); Cl4···HO52, 2.38 (1); Cl7···HO41, 2.03 (1); Cl7···HO51, 2.07 (1); Cl8···HO42, 1.99 (1); Cl9···HO21, 2.11 (1); Cl9···HO32, 2.49 (1); Cl9···HO32, 2.35 (1); Cl8···HO31, 2.03 (1); O1···HO12, 1.74 (2). Only the hydrogen atoms of the ammonium groups are shown.

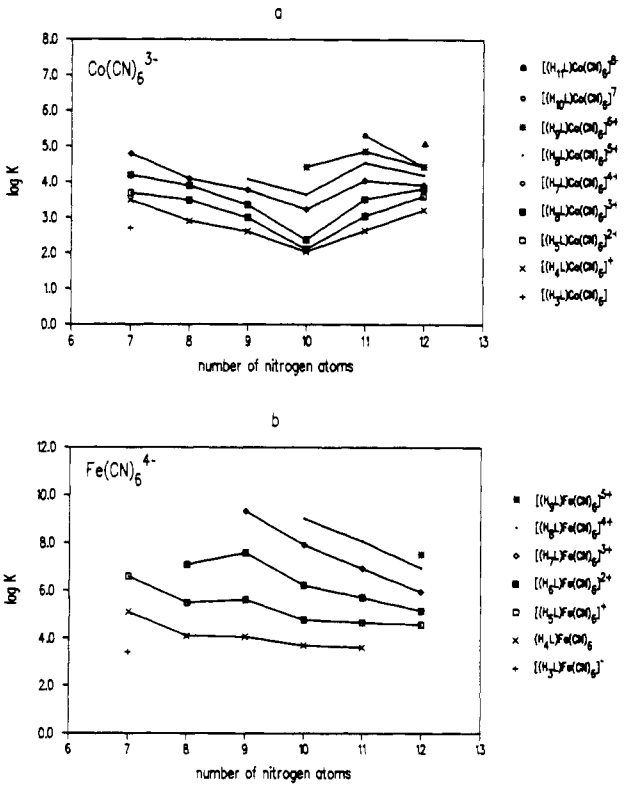


**Figure 6.** Plots of the logarithms of the equilibrium constants for the reaction of protonated $[3k]aneN_k$ ($k$ = 7–11) macrocycles with $Co(CN)_6^{3-}$ (a) and $Fe(CN)_6^{4-}$ (b) anions, respectively.

charge neutralization, which occurs with such reactions, brings about a release of water molecules from the reactants producing then an increase in translational entropy. In the case of $PdCl_4^{2-}$ anion it has been observed[7] that also the enthalpic contribution

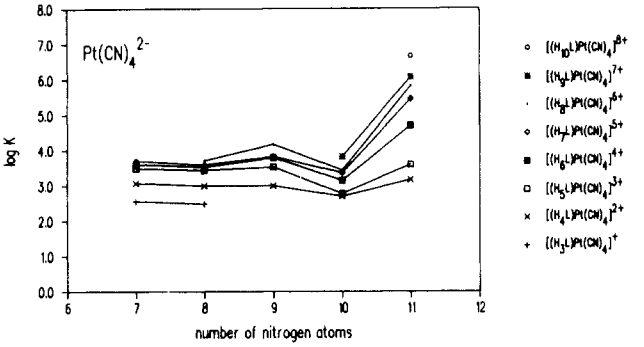


**Figure 7.** Plots of the logarithms of the equilibrium constants for the reaction of the protonated $[3k]aneN_k$ ($k$ = 7–11) macrocycles with $Pt(CN)_4^{2-}$ anion.

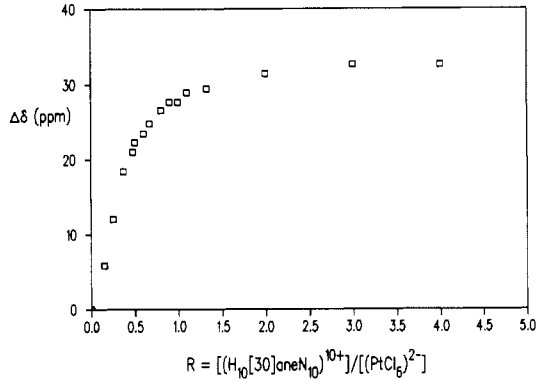


**Figure 8.** Plot of the $^{195}Pt$ NMR shift ($|\Delta\delta|$) of the $PtCl_6^{2-}$ resonance as a function of increasing $R$, where $R = [(H_{10}[30]aneN_{10})^{10+}]:[PtCl_6^{2-}]$. Spectra were recorded in 0.1 mol $dm^{-3}$ HCl solution at 298.15 K.

favors the formation of the supercomplexed species.

**(iii) Conformational Factors.** A molecular mechanics calculation performed, by using the MMX force field of PCMODEL,[18] on the isolated $(H_{10}[30]aneN_{10})^{10+}$ cations showed that the most stable macrocyclic conformation is nearly circular, being the mean diameter 12.6 (5) Å, as expected on the basis of simple electrostatic considerations. In fact this arrangement allows the nitrogen atoms to be at the maximum distances possible, since all the N–C–C–N dihedral angles are near to trans conformation. This arrangement allows the minimization of the repulsive interactions between positive charges. However the molecular structures of the $(H_{10}[30]aneN_{10})^{10+}$ cation, obtained for supercomplexed species of different anions, deviate from the circular conformation (Figure 2c–i). The actual dispositions of the fully protonated macrocycle are approximately elliptical and deviate from planarity. The intramolecular distances between symmetry-related nitrogen atoms (in all of the crystal structures $(H_{10}[30]aneN_{10})^{10+}$ is centrosymmetric) are within 8.8–12.1 Å, for the macrocyclic cation including $PdCl_4^{2-}$, 6.2–13.4 Å, for the cation interacting with $Pt(CN)_4^{2-}$, and 9.6–11.4 Å, for the cation interacting with $PtCl_6^{2-}$. In the inclusion compound of $PdCl_4^{2-}$, $(H_{10}[30]aneN_{10})^{10+}$ adopts a folded (S-shaped) conformation, as an attempt to wrap itself around the included anion (Figure 2c). Also in the other two conformations $(H_{10}[30]aneN_{10})^{10+}$ deviates from planarity, but the S-shape is less pronounced. $(H_{10}[30]aneN_{10})^{10+}$ presents a larger deviation from the circular geometry in the compound containing $Pt(CN)_4^{2-}$ than in that containing $PtCl_6^{2-}$, which involves the decacharged cation in longer contacts. The deviation from the circular shape assumed by the $(H_{10}[30]aneN_{10})^{10+}$ receptor in the crystal structures is due to the interaction with the included or surrounding anions.

As a matter of fact, the degree of protonation of the macrocycle also contributes to the determination of the molecular shape of the receptor. As shown by the crystal structure of $(H_8[30]aneN_{10})[Co(CN)_6]_2Cl_2 \cdot 10H_2O$, the conformation of the octacharged cation $(H_8[30]aneN_{10})^{8+}$ (Figure 2a,b) appears essentially imposed by the strong Coulombic repulsions between the charged nitrogen atoms, which form two very stiffened chains.[5] The intramolecular distances between symmetry-related nitrogen atoms are in the range 6.2–13.0 Å; the two unprotonated nitrogen atoms lie at 12.7 Å distance.

As far as the possibility of inclusive coordination by $(H_{10}[30]aneN_{10})^{10+}$ is considered, we can observe that the mutual dimensions of the receptor's cavity and the anion are not decisive. In fact by assuming the diameter of the sphere circumscribing the anion as a good estimation of the anion's diameter (about 4.8 Å for $Co(CN)_6^{3-}$, 4.3 Å for $PdCl_4^{2-}$ and $PtCl_6^{2-}$, 4.9 Å for $Pt(CN)_4^{2-}$)[19] and considering the hole size displayed by $(H_{10}[30]aneN_{10})^{10+}$ (2.6–9.8, 5.2–8.5, and 6.0–7.8 Å for the compounds of $Pt(CN)_4^{2-}$, $PdCl_4^{2-}$, and $PtCl_6^{2-}$, respectively), calculated as reported in ref 20, we find that, in principle, all these anions could be included into the receptor's cavity. Indeed optimization of electrostatic and hydrogen-bonding interaction between the macrocyclic receptor and the anions does not imply the localization of the anion into the macrocyclic cavity.

**Acknowledgment.** Financial support from Progetto Finalizzato di Chimica Fine e Secondaria of the Italian Research Council (CNR) is gratefully acknowledged. We are also indebted to the Spanish–Italian "Acciones Integradas" for travelling facilities.

**Registry No.** $K_3[Co(CN)_6]$, 13963-58-1; $K_2Pt(CN)_4$, 562-76-5; $K_2PtCl_6$, 16921-30-5; $K_4[Fe(CN)_6]$, 13943-58-3; $(H_7[21]aneN_7)[Pt(CN)_4]^{5+}$, 140175-42-4; $(H_8[24]aneN_8)[Pt(CN)_4]^{6+}$, 140175-43-5; $(H_8[27]aneN_9)[Pt(CN)_4]^{6+}$, 140175-44-6; $(H_9[30]aneN_{10})[Pt(CN)_4]^{7+}$, 140175-45-7; $(H_{10}[30]aneN_{10})[Pt(CN)_4]_5 \cdot H_2O$, 140175-37-7; $(H_{10}[30]aneN_{10})(PtCl_6)_2Cl_6 \cdot 2H_2O$, 140175-38-8; $(H_{10}[33]aneN_{11})[Pt(CN)_4]^{8+}$, 140175-41-3; $(H_{11}[36]aneN_{12})[Co(CN)_6]^{8+}$, 140175-39-9; $(H_9[36]aneN_{12})[Fe(CN)_6]^{5+}$, 140175-40-2.

**Supplementary Material Available:** Tables SI–SVII, listing anisotropic thermal parameters, positional parameters for the hydrogen atoms, bond distances and angles, and crystallographic and refinement data for **1** and **2** (8 pages); listings of observed and calculated structure factors for **1** and **2** (34 pages). Ordering information is given on any current masthead page.

(18) Derived from MM2 (QCPE-395, 1977) of N. L. Allinger.

(19) Anion radii have been calculated by adding the van der Waals radius of the outer atom to the crystallographic distance between the central metal ion and the outer atom.

(20) The minimum hole size of macrocyclic ligands has been estimated, on the assumption that one hydrogen atom of each ammonium group points toward the symmetry center, by subtracting twice the N–H bond distance and the van der Waals hydrogen radius from the intramolecular distances between symmetry-related nitrogen atoms. This is a reductive estimation of the hole size, as the hydrogen atoms of the ammonium groups mostly point outside the macrocyclic cavity (Figures 3 and 5).